THE ASTROPHYSICAL JOURNAL, 329:L93–L96, 1988 June 15

BOW SHOCKS AND BUBBLES ARE SEEN AROUND HOT STARS BY *IRAS*

DAVE VAN BUREN[1]
Physics Department, Johns Hopkins University and Space Telescope Science Institute
AND
RICHARD MCCRAY
Joint Institute for Laboratory Astrophysics, University of Colorado and National Bureau of Standards
Received 1987 August 17; accepted 1988 March 11

ABSTRACT

Examination of the *IRAS* all-sky imagery reveals extended, arcuate, and ringlike features associated with hot luminous stars. They fall into a number of classes: stellar wind bow shocks, stellar wind bubbles, dust shells, dust heated by isolated B stars, bright rims, and dust in H II regions. Here we discuss some objects in which the star exercises structural control over the spatial distribution of dust: bow shocks, bubbles, and radiation pressure–driven shells. We present a list of the 15 most prominent objects, show a few prototypes, and explain their characteristics in terms of thermal emission processes and gasdynamics.

Subject headings: hydrodynamics — infrared: sources — interstellar: matter — stars: early-type — stars: high-velocity — stars: winds

I. INTRODUCTION

The *IRAS* imaging presents a new opportunity to study the interactions of hot luminous stars with the material that surrounds them. Even though the typical optical depth in dust within 10 pc of a hot star is 10^{-2}, this fraction of the star's bolometric luminosity converted to the infrared is a strong *IRAS* signal. Starlight-heated dust thus provides an excellent gas tracer for regions with more or less normal dust-to-gas ratio.

In this *Letter* we discuss our "quick-look" survey of the *IRAS* imaging for 60 μm bright arcuate and ringlike features associated with hot luminous stars. We have found 15 unambiguous cases—they are obvious upon visual examination of the SkyFlux maps and do not require further processing to become apparent. Several other forms of extended infrared emission are also associated with early-type stars. Dust in H II regions is very common and provides roughly half the total IR luminosity of the galaxy. Bright rims of molecular clouds undergoing photoevaporation are prominent and will provide useful diagnostics for the mechanics of photodissociation and ionization fronts. Finally, diffuse IR from dust in the neighborhoods of B stars can be used to probe the three-dimensional structure of the interstellar medium (ISM), as will be discussed in a subsequent paper.

II. THE SURVEY

During the course of our study of dust shells associated with Galactic H II regions, we found a number of arc-shaped features at the positions of hot luminous stars. These objects are distinguished from the generally larger and cooler dust shells like that around λ Orionis, by the following:

1. Unusually high color temperature [$I(60\ \mu m)/I(100\ \mu m) > 0.3$]; and
2. Morphology of a smooth limb-brightened shell or partial shell and/or of a medium whose volume emissivity falls with distance from a center, but with a central (possibly offset) hole.

We call these objects generically "infrared ring nebulae"; some of them we can further identify as "stellar wind bow shocks," "stellar wind bubbles," and "radiation pressure–driven bow waves."

We visually examined all HCON 1 SkyFlux plates using composites of the 12 μm, 60 μm, and 100 μm images in order to find those objects which satisfy the above criteria. Our intent was to identify only the most obvious examples of infrared ring nebulae, so our survey should not be considered complete in any sense. In particular, objects were certainly missed in regions of confusion. In addition, the sensitivity of the survey to surface brightness strongly varied from plate to plate. The search turned up 33 objects, of which 15 are listed in Table 1. Of the remaining, one is a comet, two are supernova remnants, one is a strongly heated dark cloud, one is a bright rim, 12 are luminous stars embedded in wisps of cirrus, and one is a planetary nebula. The most common morphology in the list is a partial shell.

We were able to identify central OB and WR stars (in the Bright Star, SAO, and HD catalogs) for most (13 of 15) of these objects. Because of our search technique, all the objects have angular sizes of tens of arcminutes and are within a kiloparsec or so. At greater distances they will not only be smaller and less likely to be resolved but will also be more concentrated to the galactic plane, and hence more confused. The *IRAS* band fluxes presented are generally consistent with thermal dust emission with a reasonable emissivity law and a small range of dust temperatures, with the exception of the IR nebula around HD 192163 (NGC 6888), which is probably dominated by lines (§ V). Note that the fluxes reported for ζ Oph, λ Ori, and α Cam are only for a minor portion of the nebula, to facilitate comparison with the theory presented in § III. The color temperatures of the brightest portion of each nebula inferred from the 60 μm and 100 μm bands can be compared to the cirrus color temperature of 22 K (Terebey and Fich 1986). This large difference in color temperature makes them easy to pick out from a confusing background of cirrus.

Figure 1 (Plates L10–L15) shows 60 μm images of six of these objects. The first two, α Cam and ζ Oph, are the best examples of stellar wind bow shocks, stationary structures

[1] Davis Fellow.

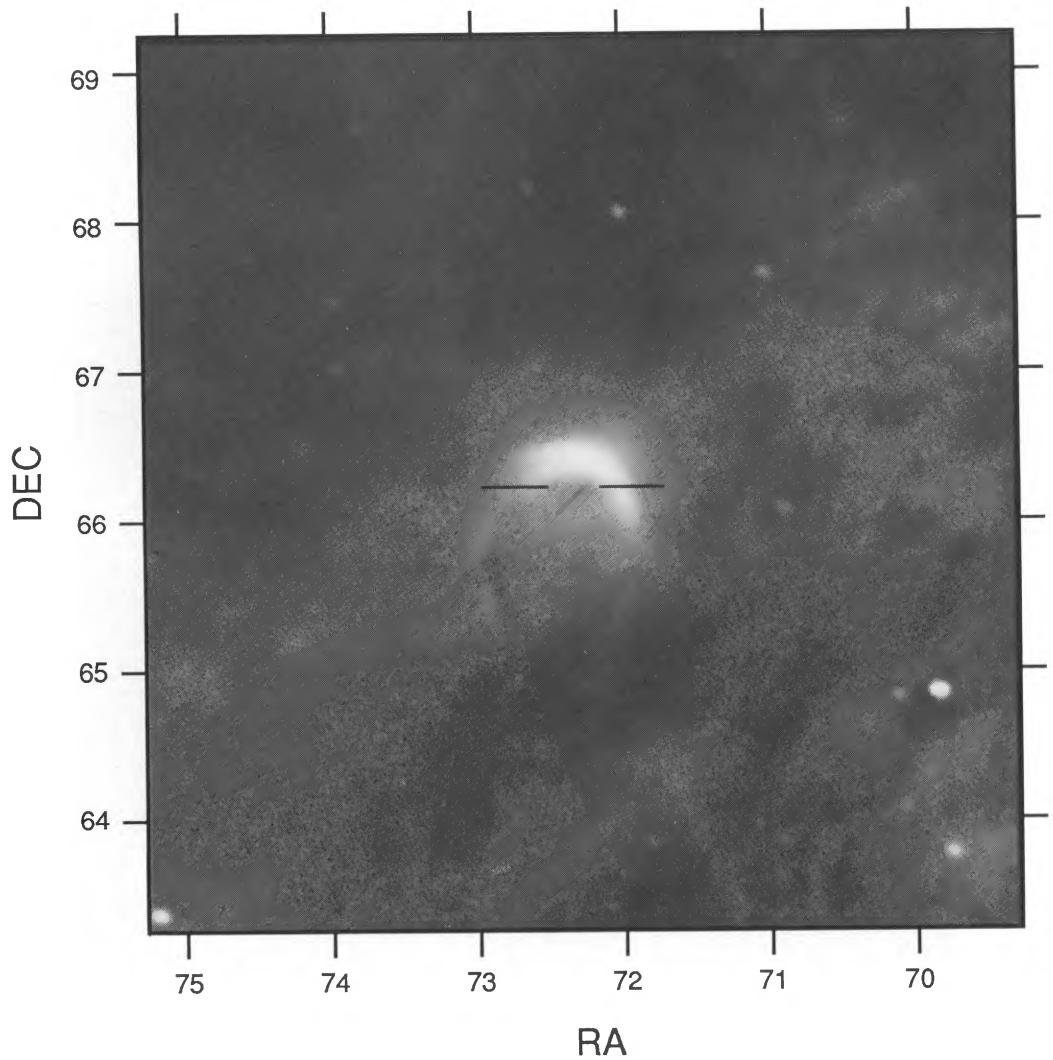

FIG. 1*a*

FIG. 1.—Six prototypical infrared ring nebula in the 60 μm band of *IRAS*. These objects are interpreted as stellar wind bow shocks, stellar wind bubbles, and radiation-pressure–driven bow waves. The positions of the central stars are indicated by tick marks and scales give both equatorial coordinates in degrees. (*a*) α Cam, bow shock; (*b*) ζ Oph, bow shock; (*c*) HD 50896 (S308), wind bubble; (*d*) HD 192163 (NGC 6888), wind bubble; (*e*) δ Sco, bow shock viewed obliquely; and (*f*) δ Per, possible radiation-pressure–driven bow wave.

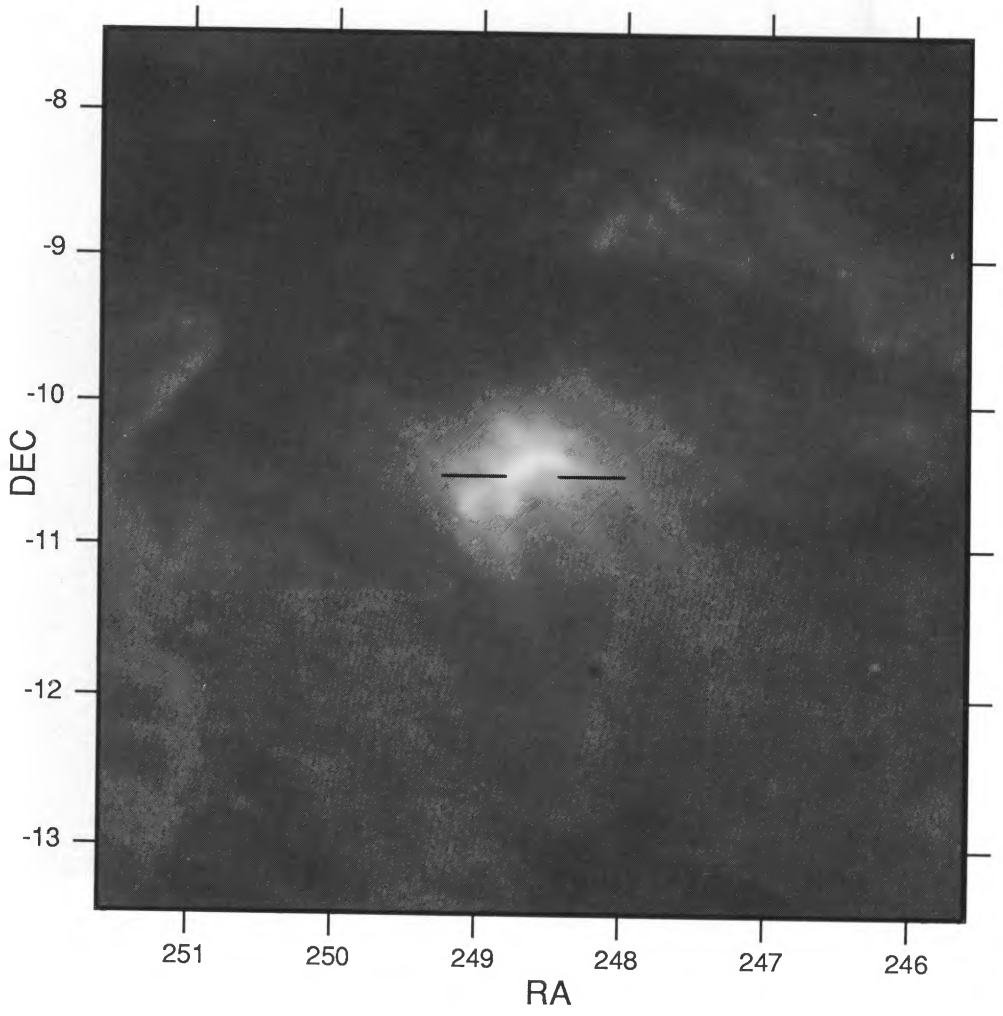

FIG. 1*b*

VAN BUREN AND MCCRAY (*see* **329**, L93)

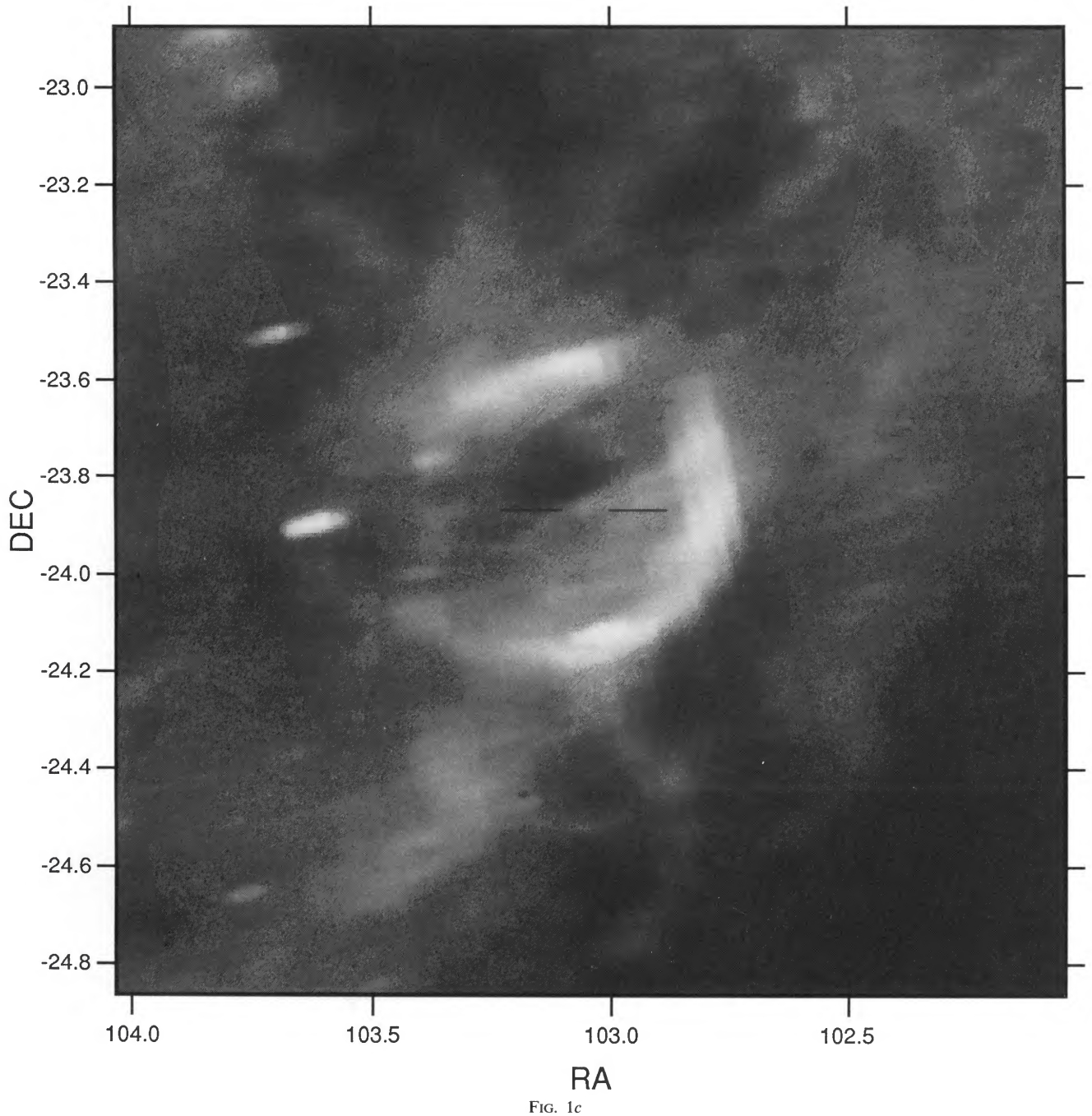

FIG. 1*c*

VAN BUREN AND MCCRAY (*see* **329**, L93)

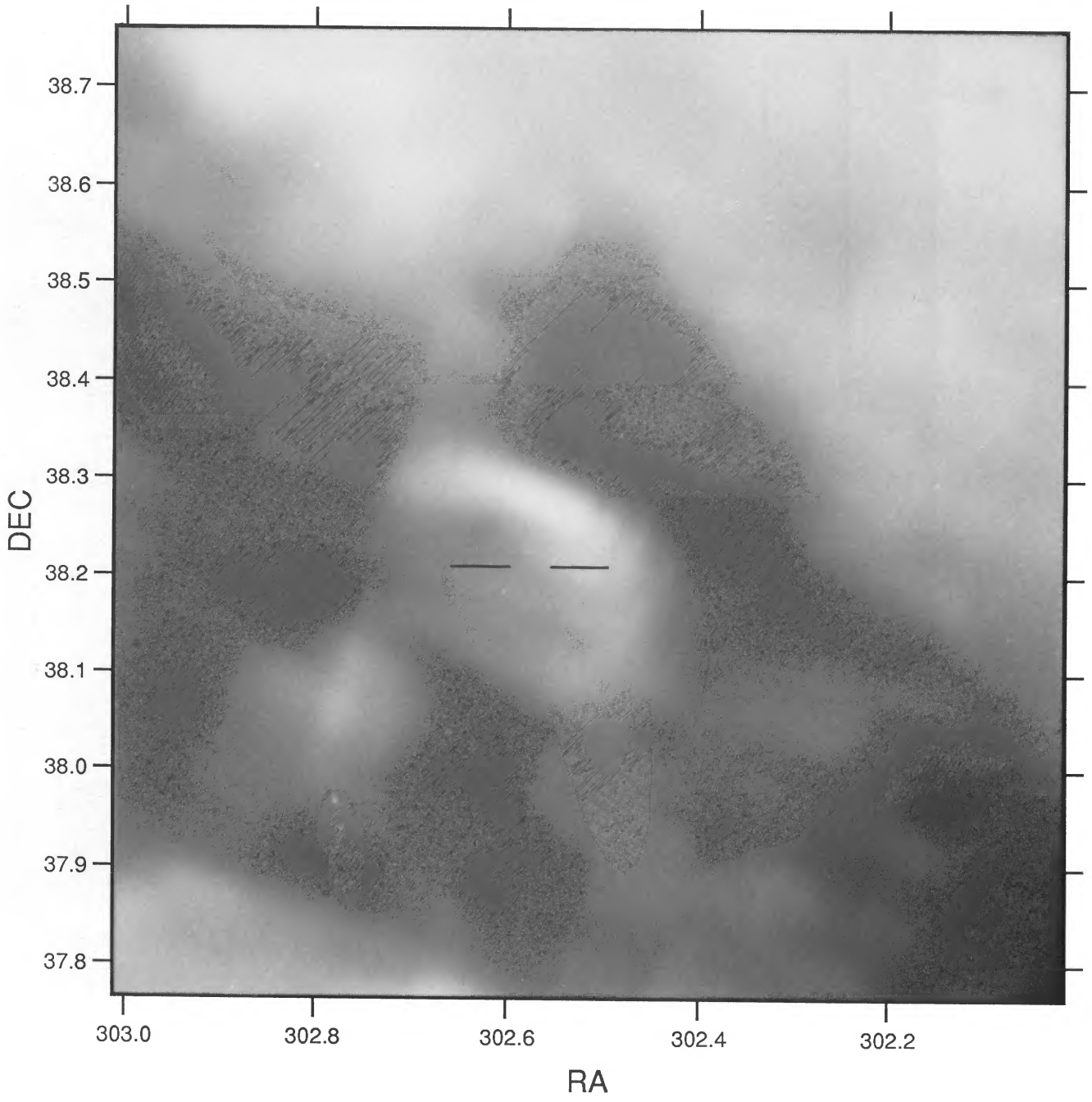

FIG. 1*d*

VAN BUREN AND MCCRAY (*see* **329**, L93)

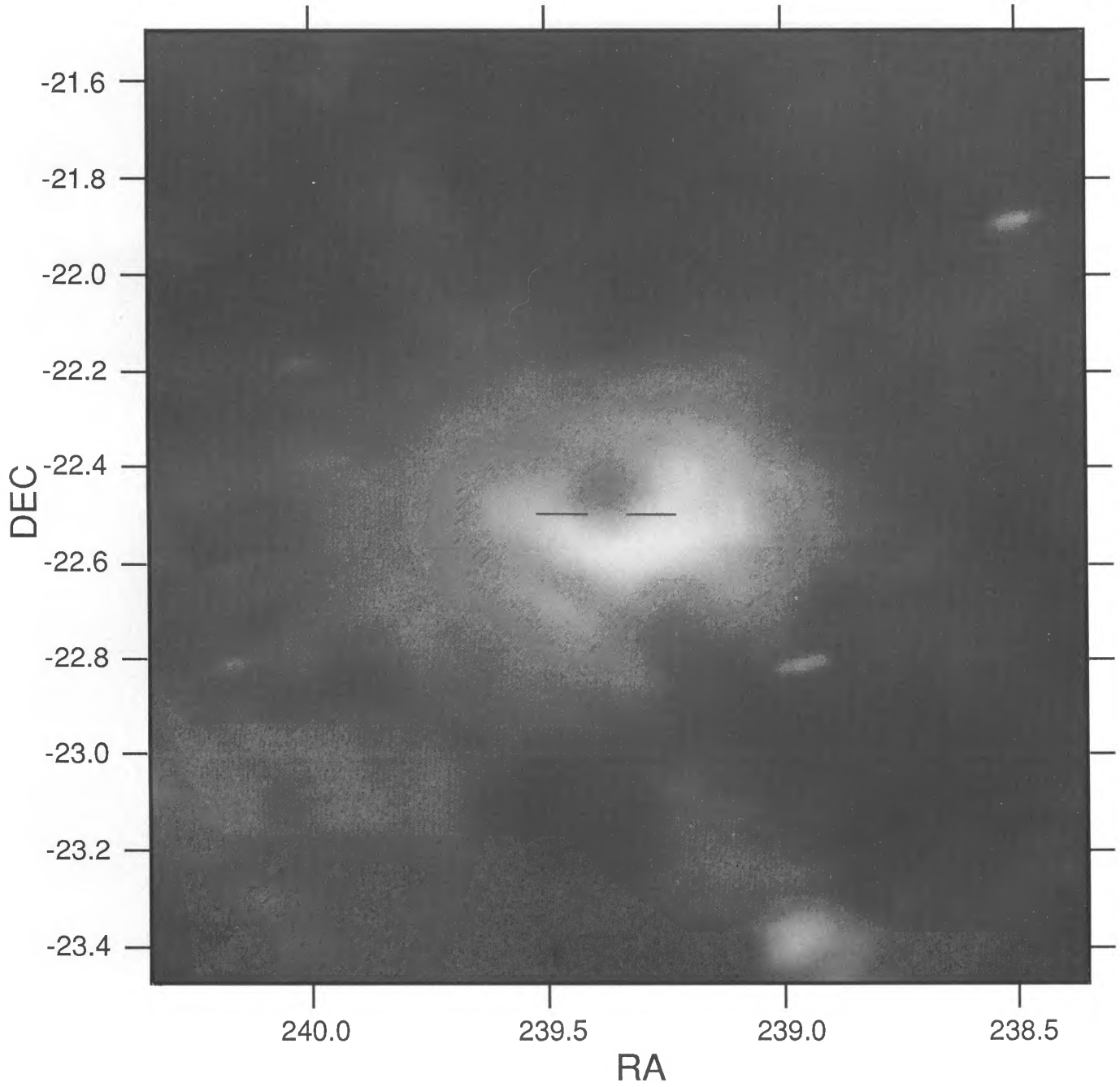

FIG. 1*e*

VAN BUREN AND MCCRAY (*see* **329**, L93)

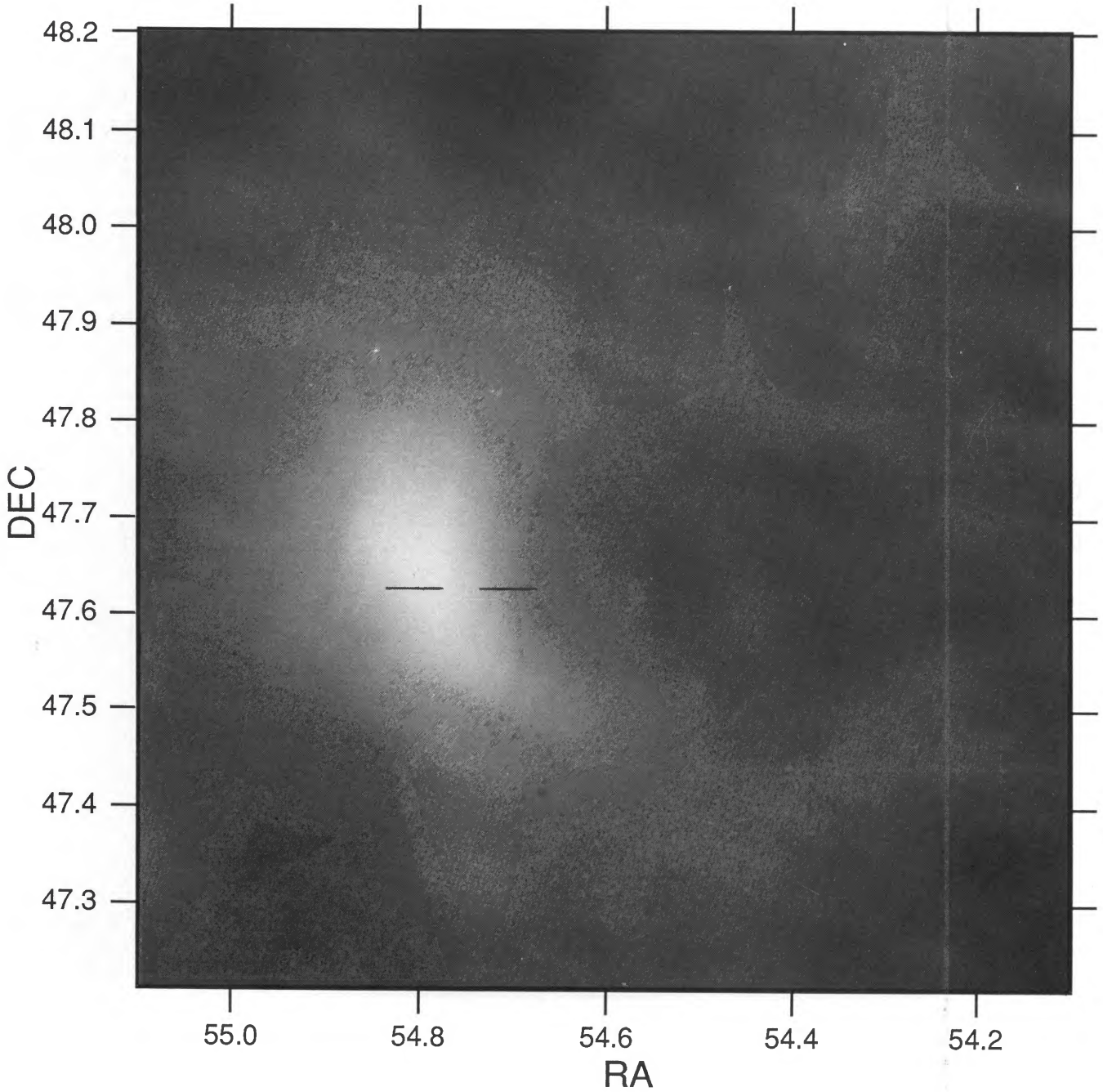

FIG. 1*f*

VAN BUREN AND MCCRAY (*see* **329**, L93)

TABLE 1

IRAS STELLAR WIND BOW SHOCKS AND BUBBLES

Star	Spectrum	Size	F_{12} (W/M^2)	F_{25} (W/M^2)	F_{60} (W/M^2)	F_{100} (W/M^2)	$T^{max}_{60/100}$ (K)	Type[a]
ζ Oph[b]	O9.5 Vn	15′ × 30′	2.8×10^{-12}	1.1×10^{-11}	9.4×10^{-11}	2.3×10^{-12}	43	⊃
HD 171491	B5	30 × 40	1.6×10^{-12}	7.5×10^{-13}	3.7×10^{-11}	3.9×10^{-12}	33	)
HD 192163[c]	WN6	25 × 15	1.7×10^{-12}	4.0×10^{-12}	8.1×10^{-12}	1.7×10^{-12}	Lines	○
U82.3[d]	...	12 × 20	2.7×10^{-11}	1.9×10^{-11}	3.7×10^{-12}	1.2×10^{-11}	26	⊃
U82.4[e]	...	50 × 49	3.1×10^{-11}	2.0×10^{-11}	8.1×10^{-11}	1.0×10^{-10}	28	⊃
6 Cep	B3 IV	45 × 60	2.6×10^{-12}	3.1×10^{-12}	8.6×10^{-12}	5.9×10^{-12}	35	⊃
λ Cep	O6 If	66 × 55	6.0×10^{-13}	1.2×10^{-11}	1.9×10^{-11}	1.5×10^{-12}	35	⊃
κ Cas	B Iae	25 × 25	9.3×10^{-13}	2.8×10^{-13}	7.9×10^{-12}	3.0×10^{-12}	43	⊃
α Cam[b]	O9.5 Iae	30 × 45	3.4×10^{-13}	1.9×10^{-12}	4.8×10^{-12}	1.9×10^{-12}	39	⊃
δ Per	B5 III	15 × 25	5.5×10^{-13}	3.6×10^{-13}	3.1×10^{-12}	1.9×10^{-12}	38	)
λ Ori[b]	O IIIf	14 × 22	2.3×10^{-13}	3.1×10^{-13}	2.4×10^{-12}	1.4×10^{-12}	33	⊃
HD 50896[f]	WN5	40 × 42	7.4×10^{-13}	6.7×10^{-13}	3.0×10^{-13}	1.9×10^{-12}	32	○
τ CMa	O9 Ib	43 × 37	5.2×10^{-12}	3.4×10^{-13}	5.4×10^{-12}	3.7×10^{-12}	30	⊃
δ Pic	B3 III + O9 V	28 × 28	1.6×10^{-13}	2.4×10^{-13}	7.2×10^{-13}	3.1×10^{-13}	34	⊃
δ Sco	B0.3 IV	90 × 94	1.5×10^{-12}	1.4×10^{-11}	3.4×10^{-11}	9.8×10^{-12}	43	⊃

[a] Key: ○ = bubble, ⊃ = bow shock,) = bow wave.
[b] Sizes and fluxes refer to leading steradian of shell only; whole object values are much larger. λ Ori values are uncertain by factor of 2 because of confusing background.
[c] Exciting star of NGC 6888.
[d] Unidentified central star, galactic coordinates $l = 82.3, b = +2.9$.
[e] Unidentified central star, galactic coordinates $l = 82.4, b = +2.3$.
[f] Exciting star of S308.

formed by the interaction between the ISM and the stellar wind of a rapidly moving star. These structures are most easily recognized when the relative velocity of the star and gas is transverse to the line of sight. In a bow shock the ridge line of infrared emission is an open parabolic arc, with the star (if identified) near the focus. The next two, S308 and NGC 6888, are examples of stellar wind bubbles, in which the star is nearly stationary relative to the ISM. They are characterized by a nearly complete ring with a more or less centered star. The fifth object, δ Sco, probably represents a bow shock, but the relative velocity has a significant component along the line of sight. As a result, the brightest part of the bow shock is not the most limb-brightened part, and so the structure is more amorphous. The last object, δ Per, may represent a radiation pressure–driven bow wave.

Most, but not all, of the objects listed have faint diffuse emission on both the Polomar red and blue prints, and a number have been observed with more sensitive instruments. Of special note is the [O III] λ5007 observation by Gull and Sofia (1979) of ζ Oph and their interpretation of the structure in terms of a stellar wind bow shock.

III. BOW SHOCKS

The prototype of this object is α Cam. This object was first discussed by de Vries (1985), who interpreted low-resolution *IRAS* data as showing a stellar wind bubble around the star. Here we argue that the structure is a bow shock instead. This interpretation removes the time dependence of the structure and yields a model whose only free parameters are the albedo and the mean size of a UV-absorbing dust grain.

Consider a star with mass-loss rate $\dot{m}_* = \dot{m}_{*,-6}\, 10^{-6}\ M_\odot\ \mathrm{yr}^{-1}$ and wind velocity $v_w = 10^8\ \mathrm{cm\ s^{-1}}\, v_{w,8}$ moving supersonically through the ISM (density $n_0\ \mathrm{cm^{-3}}$) with a velocity $v_* = v_{*,6}\, 10^6\ \mathrm{cm\ s^{-1}}$. There is then a length scale (Weaver *et al.* 1977)

$$l_1 = 1.74 \times 10^{19} \dot{m}_{*,-6}^{1/2}\, v_{w,8}^{1/2} v_{*,6}^{-1} \mu_H^{1/2} n_0^{-1/2}\ \mathrm{cm} \quad (1)$$

corresponding to the point at which the ram pressure of the free-streaming stellar wind equals that of the interstellar wind. Here μ_H is the dimensionless mean molecular weight per H atom.

The thickness of the shocked wind layer can be estimated roughly by approximating the stellar wind terminal shock and the contact discontinuity between the shocked wind and shocked ISM as concentric hemispheres. It can be shown easily that the shocked wind will not cool appreciably in the time it takes to flow around to the base of the hemisphere at a velocity of order its sound speed. Approximating the shocked wind as a gas at constant density and temperature, the continuity equation and the jump conditions give an estimate of the distance to the contact discontinuity from the star,

$$l_2 \approx (1 + 2/\sqrt{3})^{1/2} l_1 \approx 1.47 l_1\ . \quad (2)$$

The outer bow shock, which sweeps up the ambient medium, is radiative for typical stellar velocities, $v_* < 100\ \mathrm{km\ s^{-1}}$, so the density of the swept-up shell, in terms of the Mach number, is $n_{\mathrm{shell}} = \mathcal{M}^2 n_0$. Its thickness can be estimated by considering the mass flux across the outer shock and the rate at which the shocked ISM flows around the "obstruction." For analytic symplicity we approximate the shape $y(x)$ of the leading shock as a parabola: $y(x) = x^2/l_2$, where x is the transverse distance from the line connecting the star and the stagnation point. The interstellar mass flux entering the shell interior to x is then $\dot{m}_{\mathrm{shock},x} = \pi x^2 \mu_H m_H n_0 v_*$ while the flow through the shell is $2\pi x \sigma v_{\mathrm{shell},x}$, where σ is the surface density in the shell and $v_{\mathrm{shell},x}$ is the flow velocity in the x-direction. Since the shock stops only the perpendicular component of velocity, $v_{\mathrm{shell},x} = (4/3) v_* x/l_2$ (for $x \ll l_2$). Equating the two mass fluxes then gives $\sigma = \frac{3}{8} \mu_H m_H n_0 l_2$ or a column density $N = \sigma/(\mu_H m_H)$. We find

$$N = 9.6 \times 10^{18} \dot{m}_{*,-6}^{1/2}\, v_{w,8}^{1/2} \mu_H^{-1/2} n_0^{1/2} v_{*,6}^{-1}\ \mathrm{cm^{-2}} \quad (3)$$

and a thickness $\delta = \frac{3}{8} \mathcal{M}^2 l_2$. For a normal dust-to-gas ratio, this implies a total UV optical depth (using $A_{UV} = 2.2 \times 10^{-21} N$—Spitzer 1978):

$$\tau_{UV} = 0.021 \dot{m}_{*,-6}^{1/2}\, v_{w,8}^{1/2} v_{*,6}^{-1/2} \mu_H^{-1/2} n_0^{1/2} f_g\ , \quad (4)$$

where f_g is the extinction-averaged fraction of grains that survive the shock.

The standoff distance of α Cam is $l_2 = 5.1$ pc (assuming a distance of 1100 pc). Other parameters are: $L_* = 2.5 \times 10^{39}$ ergs s^{-1} and $\dot{m}_{*,-6} = 5$ (Voels *et al.* 1988), $v_{w,8} = 2.05$ (Gathier, Lamers, and Snow 1981), $v_{*,6} = 4.8$ (Stone 1979). Then, from equations (1) and (2) we infer $n_0 = 0.84$ cm^{-3} using $\mu_H = 1.4$. This is in excellent agreement with the Fabry-Perot measurements by Reynolds and Ogden (1982) of the mean density in the H II region of 0.77 cm^{-3}. Given n_0, and assuming f_g to be as large as 0.5 (McKee *et al.* 1987), we may calculate the expected infrared luminosity of the bow shock's leading steradian: $L_{IR} \approx \tau_{UV}(1 - A)L_*/4\pi = 1.1 \times 10^{36}$ ergs s^{-1}, where A = the ultraviolet albedo of the dust ~0.5. This agrees well with our measured value of $1.6 \pm 0.8 \times 10^{36}$ ergs s^{-1} derived from the co-added images in all four bands with a 60 μm/100 μm color temperature of 39 K and a λ^{-2} emissivity law (see below).

The dust temperature, and hence the *IRAS* colors, can be understood in terms of Draine and Lee's (1985) dust model. For the case of a predominantly UV radiation field, their results for the dust temperature at a distance r from the star can be written

$$T_d = 27 a_{\mu m}{}^{-1/6} L_{*,38}{}^{1/6} r_{pc}{}^{-1/3} \text{ K}, \quad (5)$$

using a dust emissivity law $j = \lambda^{-2}B(T)$. Here the dust grain has a radius $a_{\mu m}$ (μm), the star has a UV luminosity of $10^{38}L_{38}$ ergs s^{-1}, and the distance to the dust from the star is in parsecs. The observed peak color temperature of 39 K is about what we would expect from dust grains with a radius ~ 0.2 μm.

The proper motion of α Cam, as noted by de Vries (1985), is misaligned with the symmetry axis of the infrared nebula by 40°–70°. The important velocity is not the space motion relative to the LSR, but rather the star's motion with respect to the gas. If we assume the gas motion is that given by galactic rotation, then the peculiar motion of the star $\Pi_p = 0.6 \pm 5.9$ km s^{-1}, $\Theta_p = 23.2 \pm 8.5$ km s^{-1}, $Z_p = 42.4 \pm 12.1$ km s^{-1} (Stone 1979), is toward smaller galactic latitudes by more or less the amount required to remove the apparent discrepancy between the symmetry axis and the direction of proper motion.

On the Palomar prints, α Cam is associated with low surface brightness emission (red) and reflection (blue) nebulae, which map $\int n_e{}^2\, dl$ and $\int n_e r^{-2}\, dl$, respectively. These are coincident with the infrared arc of Figure 1*a*. We estimate the emission measure excess of the bow shock over the surrounding H II region to be ~60 cm^{-6} pc in the context of the model presented above. The mean emission measure of the H II region is 93 cm^{-6} pc, so the structure is near the plate limit, consistent with its appearance on the prints. The reflection nebula's surface brightness requires that the dust albedo in the blue bandpass is of order 0.1, a reasonable value. The morphologies in the blue and red are different: the red shows a much narrower arc than does the blue. This is to be expected since the compressions are highest near the apex of the bow shock, so $n_e{}^2$ is even more enhanced there, while the blue just measures the dust column, which is not as affected by the compression. Quantitative optical data would make this discussion more secure.

IV. BUBBLES

Several well-known stellar wind bubbles blown by Wolf-Rayet stars appear in the list of Table 1. Prototypical is S308, which is shown in the 60 μm band of the *IRAS* CoAdd in Figure 1. The infrared emission from this object is easily understood in terms of radiatively heated dust in the well-studied optical bubble (Kwitter 1979; Chu *et al.* 1982). Castor, McCray, and Weaver (1975) give the column density of a stellar wind bubble under the assumption of no interior radiative losses. The UV optical depth of the dust in the swept-up shell then follows:

$$\tau_{UV} = 0.066 \dot{m}_{*,-6}{}^{1/5} v_{w,8}{}^{2/5} \mu_H{}^{4/5} n_0{}^{4/5} r_{shell,pc}^{3/5} v_{shell,5}^{-3/5} f_g, \quad (6)$$

where the shell radius is in parsecs and its expansion velocity is in km s^{-1}. The infrared luminosity of the shell is then just $L_{IR} = \tau_{UV}(1 - A)L_*$. The observed IR luminosity of S308 matches this prediction for $n_0 = 4$ cm^{-3}. This is the same density that is obtained from dynamical considerations (Van Buren 1986). The relevant parameters here are $\dot{m}_{*,-6} = 33$ and $v_{w,8} = 1.7$ (Barlow, Smith, and Willis 1981); $r_{shell,pc} = 7.2$ and $v_{shell,5} = 60$ (Chu *et al.* 1982) so $f_g \approx 0.5$; $L_{*,38} = 3$ (Nussbaumer *et al.* 1982). The observed dust color temperature of 32 K can be matched with a grain radius ~0.2 μm via equation (5).

V. LINE EMISSION FROM NGC 6888

The bubble NGC 6888 also appears in Table 1 and Figure 1, but its infrared properties cannot be fitted by a model involving radiatively heated dust. Its spectrum is much too peaked at 60 μm: $I(25\ \mu m)/I(60\ \mu m) = 0.53$ while $I(60\ \mu m)/I(100\ \mu m) = 4.9$. This cannot be matched by any reasonable emissivity law for dust grains. On the other hand, the observed 60 μm to 100 μm ratio is consistent with the expected flux ratio of the O III 52 μm and 88 μm forbidden lines (Dinerstein, Lester, and Werner 1985) in NGC 6888 for the optically inferred density $n_0 \approx 10^3$ cm^{-3} (Parker 1978). We should also note the remarkable similarity of the *IRAS* 60 μm image to the [O III] λ5007 image of Parker, but it does not match the morphology in other optical lines (R. Dufour, private communication).

To verify the hypothesis that the infrared emission from NGC 6888 is dominated by lines, we examined the *IRAS* Low Resolution Spectrometer (LRS) spectrum of NGC 6888; it is shown in Figure 2. The two broad features are due to Ar III 9.0 μm and Ne III 15.5 μm. The line broadening is caused by the spatial extension of the source. The ratio of the line intensities, $I(15.5\ \mu m)/I(9.0\ \mu m) \approx 8:1$ is typical of that observed in planetary nebulae (Pottasch *et al.* 1984). Assuming that the 52 μm line dominates the flux in the *IRAS* 60 μm band, we obtain $I(52\ \mu m)/I(15.5\ \mu m) \approx 3:1$. For comparison, $I(52\ \mu m)/I(15.5\ \mu m) \approx 1:1$ in the planetary nebula NGC 6543 according to the data of Pottasch *et al.* and Dinerstein, Lester, and Werner.

NGC 6888 is unique among these objects because it has a high pressure, $nT \approx 10^7$ cm^{-6} K. Since the line emissivity is proportional to n^2 while the dust emissivity only goes as n, one expects that higher pressure objects will be increasingly dominated by emission lines in the infrared.

The presence of line emission in the *IRAS* bands from NGC 6888 raises the possibility that the other objects listed in the table have lines contaminating their fluxes as well. The [O III] lines are major coolants and can, in principle, reradiate of order 1% of the stellar ionizing continuum. This roughly matches the energetics of the dust emission, so the dust temperatures in Table 1 for at least ζ Oph and HD 50896, both of which show prominent λ5007 emission, should be viewed with caution. Precise determination of dust temperatures will

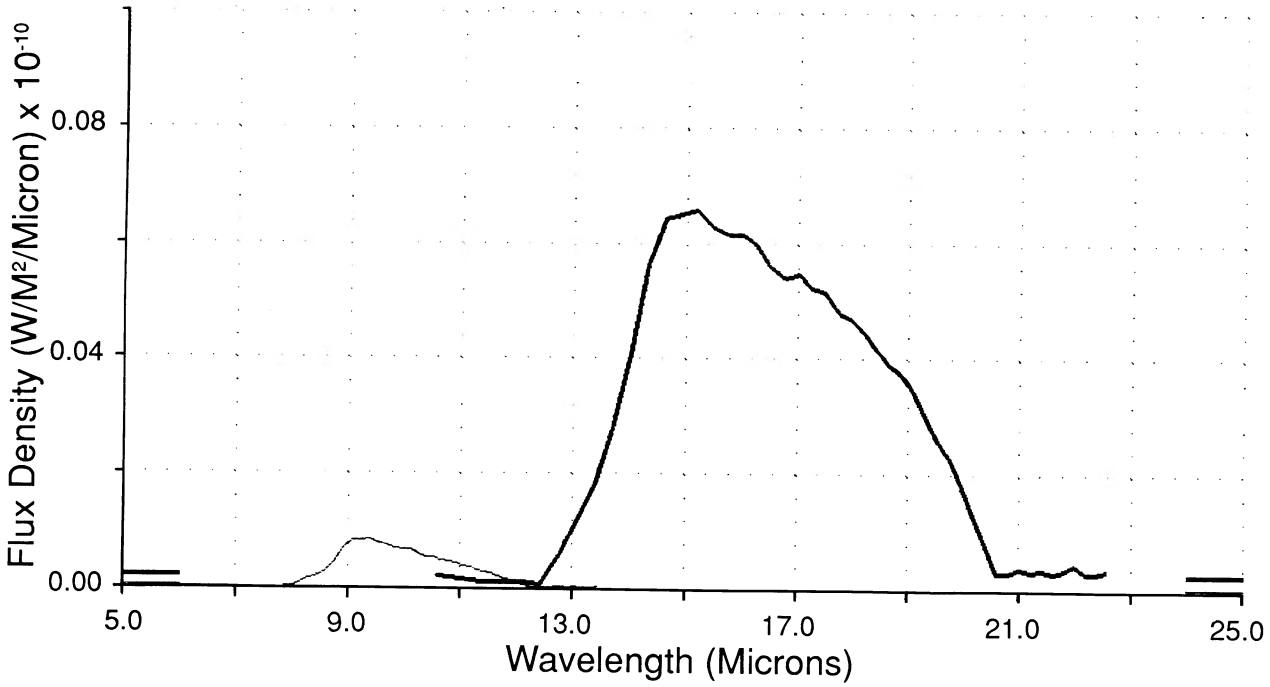

FIG. 2.—*IRAS* LRS spectrum of NGC 6888. The two broad features are the 9.0 μm line of Ar III and the 15.5 μm line of Ne III. These are typical lines found in high-excitation planetary nebulae. The broadening is caused by the extent of the source.

require airborne spectroscopy to find the contributions from lines.

VI. RADIATION-PRESSURE–DRIVEN BOW WAVES

Several of the listed objects are illuminated by stars whose expected wind momentum flux is quite small, as much as four orders of magnitude less than that of α Cam. A wind-driven bow shock model is thus not likely to account for the observed scale of the arcs. One possibility is that the momentum balance is between the stellar radiation pressure acting on dust and the oncoming interstellar wind instead. For such an object,

$$r_{\rm pc} = 1.1 \times 10^{-1} L_{36}\, \mu_{\rm H}{}^{-1} v_{*,5}{}^{-2}\,, \qquad (7)$$

where the velocity of the star with respect to the ambient medium is now in km s^{-1} and we have assumed a normal dust-to-gas ratio. Note that stars moving *slowly* can create structures with sizes of order 1 pc. Using $\dot{m}_{*,-6} = 2.7 \times 10^{-3} L_{36}{}^{5/4}$ (Van Buren 1985) it is easy to show that structures around main-sequence stars later than B3 in a unit density medium moving at 1 km s^{-1} are controlled by radiation pressure rather than winds.

This work was performed as part of the *IRAS* General Investigator Program under contract with the Jet Propulsion Laboratory of the California Institute of Technology. We would like to thank the staff at IPAC in Pasadena for their hospitality; T. Soifer, N. Gautier, D. Watson, C. McKee, and B. Savage for useful discussions; and the referee for her or his suggestions for improving the paper.

REFERENCES

Barlow, M. J., Smith, L. J., and Willis, A. J. 1981, *M.N.R.A.S.*, **196**, 101.
Castor, J., McCray, R., and Weaver, R. 1975, *Ap. J. (Letters)*, **200**, L107.
Chu, Y.-H., Gull, T. R., Treffers, R. R., Kwitter, K. B., and Troland, T. H. 1982, *Ap. J.*, **254**, 562.
de Vries, C. P. 1985, *Astr. Ap.*, **150**, L15.
Dinerstein, H. L., Lester, D. F., and Werner, M. W. 1985, *Ap. J.*, **291**, 561.
Draine, B., and Lee, H. M. 1985, *Ap. J.*, **285**, 89.
Gathier, R., Lamers, H. J. G. L. M., and Snow, T. P. 1981, *Ap. J.*, **247**, 173.
Gull, T. R., and Sofia, S. 1979, *Ap. J.*, **230**, 782.
Kwitter, K. B. 1979, Ph.D. thesis, University of California, Los Angeles.
McKee, C. F., Hollenbach, D. J., Seab, C. G., and Tielens, A. G. G. M. 1987, *Ap. J.*, **318**, 674.
Nussbaumer, H., Schmutz, W., Smith, L. J., and Willis, A. J. 1982, *Astr. Ap. Suppl.*, **47**, 257.
Parker, R. A. R. 1978, *Ap. J.*, **224**, 873.
Pottasch, S. R., *et al.* 1984, *Ap. J. (Letters)*, **278**, L33.
Reynolds, R. J., and Ogden, P. M. 1982, *A.J.*, **87**, 306.
Spitzer, L., Jr. 1978, *Physical Processes in the Interstellar Medium* (New York: Wiley).
Stone, R. C. 1979, *Ap. J.*, **232**, 520.
Terebey, S., and Fich, M. 1986, *Ap. J. (Letters)*, **309**, L73.
Van Buren, D. 1985, *Ap. J.*, **294**, 567.
———. 1986, *Ap. J.*, **306**, 538.
Voels, S., Bohannan, B., Abbott, D., and Hummer, D. 1988, *Ap. J.*, submitted.
Weaver, R., McCray, R., Castor, J., Shapiro, P., and Moore, R. 1977, *Ap. J.*, **218**, 377.

RICHARD McCRAY: Joint Institute for Laboratory Astrophysics, Boulder, CO 80309

DAVE VAN BUREN: Space Telescope Science Institute, Baltimore, MD 21218